Uniquely Shaped Double-Decker BuckyferrocenesDistinct Electron Donor –Acceptor Interactions

ARTICLE *in* JOURNAL OF THE AMERICAN CHEMICAL SOCIETY · NOVEMBER 2008

Impact Factor: 12.11 · DOI: 10.1021/ja8013902 · Source: PubMed

8 AUTHORS, INCLUDING:

Renata Marczak
Friedrich-Alexander-University of Erlangen…
21 PUBLICATIONS **419** CITATIONS
SEE PROFILE

Mateusz Wielopolski
ETH Zurich
36 PUBLICATIONS **968** CITATIONS
SEE PROFILE

Shankara Gayathri Radhakrishnan
University of Pretoria
29 PUBLICATIONS **916** CITATIONS
SEE PROFILE

Kazukuni Tahara
Osaka University
76 PUBLICATIONS **2,360** CITATIONS
SEE PROFILE

J|A|C|S
ARTICLES

Published on Web 11/12/2008

Uniquely Shaped Double-Decker Buckyferrocenes—Distinct Electron Donor−Acceptor Interactions

Renata Marczak,[†] Mateusz Wielopolski,[†] S. Shankara Gayathri,[†] Dirk M. Guldi,*[,†] Yutaka Matsuo,*[,‡] Keiko Matsuo,[‡] Kazukuni Tahara,[§] and Eiichi Nakamura*[,‡,§]

Department of Chemistry and Pharmacy & Interdisciplinary Center for Molecular Materials, Friedrich-Alexander-Universität Erlangen-Nürnberg, Egerlandstrasse 3, 91058 Erlangen, Germany, Nakamura Functional Carbon Cluster Project, ERATO, Japan Science and Technology Agency, Hongo, Bunkyo-ku, Tokyo 113-0033, Japan, and Department of Chemistry, The University of Tokyo, Hongo, Bunkyo-ku, Tokyo 113-0033, Japan

Received February 29, 2008; E-mail: guldi@chemie.uni-erlangen.de; matsuo@chem.s.u-tokyo.ac.jp; nakamura@chem.s.u-tokyo.ac.jp

Abstract: Quantum chemical calculations and various photophysical techniques, ranging from steady-state absorption and steady-state as well as time-resolved fluorescence to femtosecond pump-probe experiments, were employed to examine ground- and excited-state interactions in a set of novel double-decker buckyferrocenes (i.e., $Fe_2(C_{60}Me_{10})Cp_2$): C_{2v} and D_{5d} isomers. When compared to the individual reference systems, the intimate fullerene/ferrocene contacts reflect appreciable ground-state interactions, namely, substantial redistribution of charge density between the two electron donors (i.e., ferrocenes) and the electron acceptor (i.e., fullerene). Furthermore, an intervalence charge-transfer transition (i.e., ferrocene−ferrocenium interaction) was established, but only in the C_{2v} isomer. The first insight into the electron donor−acceptor interactions came from inspecting the fullerene-centered fluorescence. Relative to the reference compounds that contain no ferrocene, which exhibit quantum yields of up to 0.1, and knowing that the fluorescence of the investigated double-decker type conjugates is quenched to 10^{-3}, transient absorption measurements prove unequivocally the rapid formation of the radical ion-pair states as the dominant products of excited-state deactivation in the double-decker buckyferrocenes. Despite these products having much higher lying radical ion-pair states relative to the corresponding single-decker buckyferrocene, their lifetimes, which vary between 12 and 39 ps, are slightly shorter.

Introduction

Donor−acceptor dyads capable of undergoing photoinduced energy or electron transfer are of current interest in areas of light-induced electron-transfer chemistry and solar-energy conversion.[1] Fullerenes, a unique class of spherical compounds,[2] have been shown to be outstanding candidates for electron acceptors due to their low reduction potentials,[3] three-dimensional structure,[4] and small reorganization energy in electron-transfer reactions.[5] As an electron donor, on the other hand, ferrocene and its derivatives have been integrated together with an electron-accepting fullerene in various donor−acceptor conjugates.[6−8] These compositions have been used to fine-tune

[†] Friedrich-Alexander-Universität Erlangen-Nürnberg.
[‡] Japan Science and Technology Agency.
[§] The University of Tokyo.

(1) (a) Imahori, H.; Sakata, Y. *Adv. Mater.* **1997**, *9*, 537. (b) Prato, M. *J. Mater. Chem.* **1997**, *7*, 1097. (c) Martin, N.; Sánchez, L.; Illescas, B.; Pérez, I. *Chem. Rev.* **1998**, *98*, 2527. (d) Imahori, H.; Sakata, Y. *Eur. J. Org. Chem.* **1999**, 2445. (e) Diederich, F.; Gómez-López, M. *Chem. Soc. Rev.* **1999**, *28*, 263. (f) Guldi, D. M. *Chem. Commun.* **2000**, 321. (g) Reed, C. A.; Bolskar, R. D. *Chem. Rev.* **2000**, *100*, 1075. (h) Gust, D.; Moore, T. A.; Moore, A. L. *J. Photochem. Photobiol. B* **2000**, *58*, 63. (i) Gust, D.; Moore, T. A.; Moore, A. L. *Acc. Chem. Res.* **2001**, *34*, 40. (j) Guldi, D. M.; Martin, N. *J. Mater. Chem.* **2002**, *12*, 1978. (k) Guldi, D. M. *Chem. Soc. Rev.* **2002**, *31*, 22. (l) Imahori, H.; Mori, Y.; Matano, Y. *J. Photochem. Photobiol. C* **2003**, *4*, 51. (m) Nierengarten, J. F. *Top. Curr. Chem.* **2003**, *228*, 87. (n) Guldi, D. M. *Pure Appl. Chem.* **2003**, *75*, 1069. (o) El-Khouly, M. E.; Ito, O.; D'Souza, F. *J. Photochem. Photobiol. C* **2004**, *5*, 79. (p) Guldi, D. M.; Prato, M. *Chem. Commun.* **2004**, 2517. (q) Guldi, D. M. *J. Phys. Chem. B* **2005**, *109*, 11432.

(2) (a) Kroto, H. W.; Heath, J. R.; O'Brien, S. C.; Curl, R. F.; Smalley, R. E. *Nature* **1985**, *318*, 162. (b) Haddon, R. C.; Brus, L. E.; Raghavachari, K. *Chem. Phys. Lett.* **1986**, *131*, 165. (c) Kroto, H. W. *Nature* **1987**, *329*, 529. (d) Krätschmer, W.; Lamb, L. D.; Fostiropoulos, K.; Huffman, D. R. *Nature* **1990**, *347*, 354. (e) Weaver, J. H. *Acc. Chem. Res.* **1992**, *25*, 143. (f) Morton, J. R.; Negri, F.; Preston, K. F. *Acc. Chem. Res.* **1998**, *31*, 63.

(3) Xie, Q.; Perez-Cordero, E.; Echegoyen, L. *J. Am. Chem. Soc.* **1992**, *114*, 3978.

(4) *Fullerenes and Related Structures*; Hirsch, A., Ed.; Springer: Berlin, 1999; Vol. 199.

(5) (a) Imahori, H.; Hagiwara, K.; Akiyama, T.; Aoki, M.; Taniguchi, S.; Okada, T.; Shirakawa, M.; Sakata, Y. *Chem. Phys. Lett.* **1996**, *263*, 545. (b) Guldi, D. M.; Asmus, K.-D. *J. Am. Chem. Soc.* **1997**, *119*, 5744. (c) Fukuzumi, S.; Ohkubo, K.; Imahori, H.; Guldi, D. M. *Chem. Eur. J.* **2003**, *9*, 1586. (d) Guldi, D. M. *Spectrum* **2003**, *16*, 8.

(6) (a) Guldi, D. M.; Maggini, M.; Scorrano, G.; Prato, M. *J. Am. Chem. Soc.* **1997**, *119*, 974. (b) Herranz, A. M.; Illescas, B.; Martin, N. *J. Org. Chem.* **2000**, *65*, 5728. (c) Imahori, H.; Guldi, D. M.; Tamaki, K.; Yoshida, Y.; Luo, Ch.; Sakata, Y.; Fukuzumi, S. *J. Am. Chem. Soc.* **2001**, *123*, 6617. (d) Imahori, H.; Tamaki, K.; Araki, Y.; Sekiguchi, Y.; Ito, O.; Sakata, Y.; Fukuzumi, S. *J. Am. Chem. Soc.* **2002**, *124*, 5165.

(7) (a) Guldi, D. M.; Imahori, H.; Tamaki, K.; Kashiwagi, Y.; Yamada, H.; Sakata, Y.; Fukuzumi, S. *J. Phys. Chem. A* **2004**, *108*, 541. (b) Hauke, F.; Hirsch, A.; Liu, S.-G.; Echegoyen, L.; Swartz, A.; Luo, Ch.; Guldi, D. M. *ChemPhysChem* **2002**, *3*, 195.

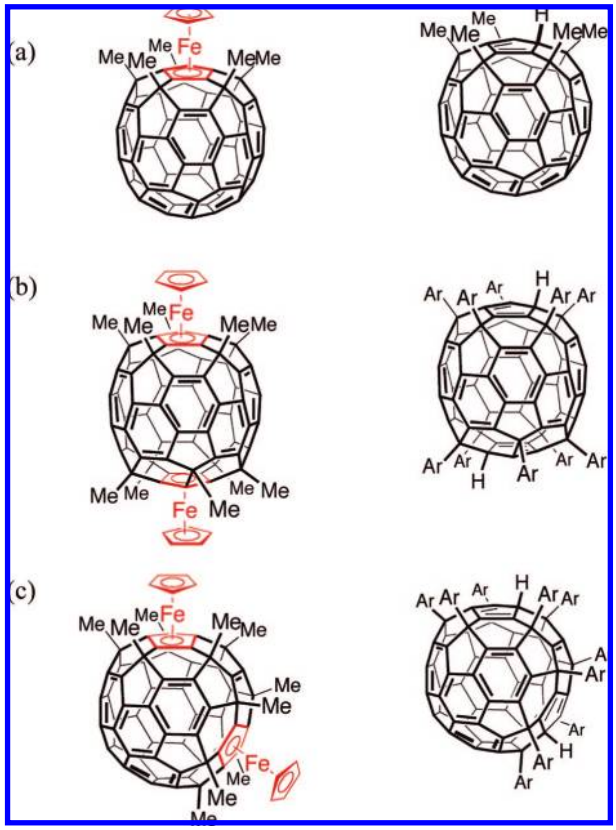

Figure 1. Structural formulas of (a) single-decker buckyferrocene, $Fe(C_{60}Me_5)Cp$, and the respective reference compound, $C_{60}Me_5H$, and (b) highly symmetric D_{5d} and (c) lower symmetric C_{2v} double-decker buckyferrocenes, $Fe_2(C_{60}Me_{10})Cp_2$, and their respective reference compounds, $C_{60}Ar_{10}H_2$ (Ar = C_6H_4-*n*Bu).

the electronic coupling, orientation, and separation between donor and acceptor sites and the total reorganization energy.[1] All these parameters are vital since they have a great impact on the rates, yields, and lifetimes of the highly energetic charge-separated states. In this context, decreasing, for example, the spacer length between the donor and acceptor moieties lead to an increase of the electronic coupling, and consequently shorter lifetimes of the charge-separated states are noted.[7,8] In our previous investigation,[8] the results obtained during photophysical characterization of ferrocene/fullerene conjugates (i.e., single-decker buckyferrocenes) were presented. In the corresponding donor−acceptor conjugates, the effective donor−acceptor distances (i.e., edge-to-edge) were completely reduced. In particular, both the fullerene and the ferrocene share a pentagon and hence are fused together (Figure 1). In these single-decker buckyferrocene conjugates, the intimate contacts between the fullerenes and the ferrocenes result in appreciable ground- as well as excited-state interactions, suggesting a substantial shift of charge density from the electron donor (i.e., ferrocene) to the electron acceptor (i.e., fullerene).

Herein, we take the uniquely shaped buckyferrocenes to the next level and report the physicochemical properties of a novel series of conjugates, where now one fullerene shares two pentagons with two ferrocenes, $Fe_2(C_{60}Me_{10})Cp_2$, instead of just one pentagon. These conjugates are termed double-decker buckyferrocenes. In particular, we have focused on the characterization of two isomers of the double-decker buckyferrocenes conjugates, that is, a previously reported, highly symmetric D_{5d} isomer and the newly synthesized, lower symmetric C_{2v} analogue (see Figure 1), to fine-tune charge-transfer and intervalence charge-transfer transitions.

Experimental Section

Materials. Double-decker buckyferrocene, D_{5d}-$Fe_2(C_{60}Me_{10})Cp_2$, was synthesized according to the method described in our previous paper.[9] The reference compound decaaryl[60]fullerenes ($C_{60}Ar_{10}H_2$), buckyferrocene, $Fe(C_{60}Me_5)Cp$, and its reference, $C_{60}Me_5H$, were prepared according to the previous paper.[12] All experiments except for the X-ray crystallography were performed with the singly chromatographed materials.

Synthesis of Double-Decker Buckyferrocene, C_{2v}-$Fe_2(C_{60}Me_{10})Cp_2$. To a white suspension of $CuBr\cdot SMe_2$ (1.85 g, 9.00 mmol) in pyridine (15 mL) was added a solution of MeMgBr (1.0 M in THF, 9.0 mL, 9.0 mmol) at 25 °C. A solution of $Fe(C_{60}Me_5)Cp$ (137 mg, 0.150 mmol) in *o*-dichlorobenzene (20 mL) was transferred to the resulting yellow suspension though a cannula. After stirring for 24 h at 25 °C, the reaction was quenched with saturated NH_4Cl (aqueous) (0.10 mL). The mixture was diluted with toluene (50 mL) and filtered though a pad of silica gel. *o*-Dichlorobenzene and other volatile materials were removed with vacuum distillation. To the residue were added $[CpFe(CO)_2]_2$ (265 mg, 0.75 mmol) and benzonitrile (20 mL). After being stirred for 3 h at 180 °C, the mixture was diluted with toluene (50 mL) and filtered though a pad of silica gel. An orange-colored solution was concentrated to a small volume and subjected to separation by HPLC (Nacalai Tesque, Buckyprep, 250 mm, hexane:toluene = 7:3). The fractions containing D_{5d}-$Fe_2(C_{60}Me_{10})Cp_2$ and C_{2v}-$Fe_2(C_{60}Me_{10})Cp_2$ were collected separately and concentrated to a small volume. Precipitation with methanol afforded both the D_{5d} compound (5.0 mg, 3% yield) and the C_{2v} compound (3.3 mg, 2% yield). Pure crystals of D_{5d} and C_{2v} compounds were obtained by slow diffusion of methanol into a solution of the compounds. Spectral data for the D_{5d} compound have been reported our previous paper.[9]

IR (ReactIR 1000, diamond probe): 3103, 2958, 2917, 2854, 1441, 1372, 1179, 1158, 1108, 1052, 998, 812, 740, 689, 688 cm^{-1}. ^1H NMR ($CDCl_3$, 500 MHz): δ 1.85 (s, 12H, CH_3), 2.25 (s, 12H, CH_3), 2.49 (s, 6H, CH_3), 4.53 (s, 10H, C_5H_5). ^{13}C NMR ($CDCl_3$, 125 MHz): δ 29.0 (4C, CH_3), 29.7 (4C, CH_3), 30.5 (2C, CH_3), 46.3 (4C, C_{60}), 49.3 (4C, C_{60}), 49.9 (2C, C_{60}), 68.0 (10C, C_5H_5), 88.4 (4C, Cp(C_{60})), 91.0 (2C, Cp(C_{60})), 91.5 (4C, Cp(C_{60})), 144.6 (4C, C_{60}), 145.9 (2C, C_{60}), 147.0 (4C, C_{60}), 147.7 (4C, C_{60}), 148.1 (4C, C_{60}), 148.8 (4C, C_{60}), 149.2 (4C, C_{60}), 149.9 (2C, C_{60}), 155.2 (4C, C_{60}), 157.4 (4C, C_{60}), 158.9 (4C, C_{60}). UV−vis (in THF): λ_{max} (ϵ) 250 (65 000), 294 (57 500), 366 (33 000), 456 (7500) nm. APCI-TOF MS: *m*/*z* calcd for $C_{80}H_{40}{}^{56}Fe_2$ (M^+), 1112.18938; found, 1112.18342.

X-ray Crystallographic Analysis of C_{2v}-$Fe_2(C_{60}Me_{10})Cp_2$. The data set was collected on a MacScience DIP2030 imaging plate diffractometer using Mo Kα (graphite monochromated, $\lambda = 0.71069$ Å) radiation. The structure was solved by the directed method (SIR97). The positional and thermal parameters of non-hydrogen atoms were refined anisotropically on F^2 by the full-matrix least-squares method, using SHELXL-97. Hydrogen atoms were placed at calculated positions and refined with a riding mode on their corresponding carbon atoms. Crystal system, monoclinic; space group, *C*2/*c* (No. 15); *R*, R_w ($I > 2\sigma(I)$) = 0.063, 0.165; *R*1, *wR*2 (all data) = 0.084, 0.183; GOF on F^2, 1.036; *T*, 173(2) K.

Quantum Chemical Calculations. Calculations were performed using the GAUSSIAN 03 program package.[10] Molecular properties

(8) (a) Guldi, D. M.; Rahman, G. M. A.; Marczak, R.; Matsuo, Y.; Yamanaka, M.; Nakamura, E. *J. Am. Chem. Soc.* **2006**, *128*, 9420. (b) Matsuo, Y.; Matsuo, K.; Nanao, T.; Marczak, R.; Gayathri, S. S.; Guldi, D. M.; Nakamura, E. *Chem. Asian J.* **2008**, *3*, 841.

(9) Matsuo, Y.; Tahara, K.; Nakamura, E. *J. Am. Chem. Soc.* **2006**, *128*, 7154.

(10) Frisch, M. J.; et al. *Gaussian 03*, Gaussian, Inc.: Wallingford, CT, 2004.

Scheme 1

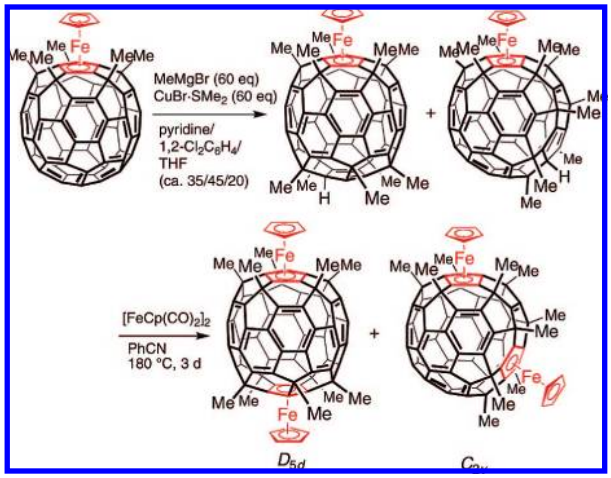

in the electronic ground state were computed using the hybrid B3PW91 DFT method. To obtain the molecular orbital schemes, all structures were optimized under the corresponding symmetry using the LANL2DZ all-electron basis set for the iron atoms and the 6-31G* basis set for carbon and hydrogen. Further single-point calculations were performed at the B3PW91/6-311+G** level of theory and LANL2DZ pseudopotentials were computed for iron in order to obtain the molecular-orbital energies.

Spectroscopic Characterization. UV−vis spectra were recorded with a Perkin-Elmer Lambda 2 spectrophotometer. Steady-state fluorescence studies were carried out with a Fluoromax 3 (Horiba) instrument. Fluorescence lifetimes were measured with a Laser Strobe fluorescence lifetime spectrometer (Photon Technology International) with 337-nm laser pulses from a nitrogen laser fiber coupled to a lens-based T-formal sample compartment equipped with a stroboscopic detector. Femtosecond transient absorption studies were performed using the 387 nm laser pulses of 150 fs pulse width of 150 nJ energy, generated by a beta-barium borate crystal upon higher order nonlinear processes from an amplified Ti:sapphire laser system (CPA 2001 Laser, Clark-MXR Inc.). The white light was generated by a 2 mm sapphire crystal, and with the help of a delay line, a time delay between the pump and the probe beams was created with a high precision. Finally, the change in optical density (ΔOD) was measured against the wavelength in both visible and near-infrared regions. Nanosecond laser flash photolysis experiments were performed with 337 nm laser pulses from a nitrogen laser (8 ns pulse width) in front-face excitation geometry.

Results and Discussion

For the synthesis of the double-decker buckyferrocenes D_{5d}- and C_{2v}-$Fe_2(C_{60}Me_{10})Cp_2$, we employed a stepwise pentamethylation of C_{60} and subsequent complexation (Scheme 1). In this regard, the methylcopper reagent, which was derived from MeMgBr and CuBr·SMe_2, was treated with the pentamethyl buckyferrocene $Fe(C_{60}Me_5)Cp$ in a mixed solvent of pyridine, THF, and *o*-dichlorobenzene to produce a mixture of regioisomers of $Fe(C_{60}Me_{10}H)Cp$, and then this precursor reacted with $[FeCp(CO)_2]_2$ in PhCN at 180 °C to obtain a mixture of regioisomers of the D_{5d}- and C_{2v}-decamethyl double-decker buckyferrocenes. HPLC separation by the use of the Buckyprep column was conducted to obtain pure D_{5d} and C_{2v} compounds.

Both the isomers were characterized by ^1H and ^{13}C NMR, high-resolution APCI-TOF mass spectra, and X-ray single-crystal analyses. Figure 2 reports the molecular structure of C_{2v}-$Fe_2(C_{60}Me_{10})Cp_2$, while that of D_{5d}-$Fe_2(C_{60}Me_{10})Cp_2$ has already been reported.[9] The distance between two iron atoms for the

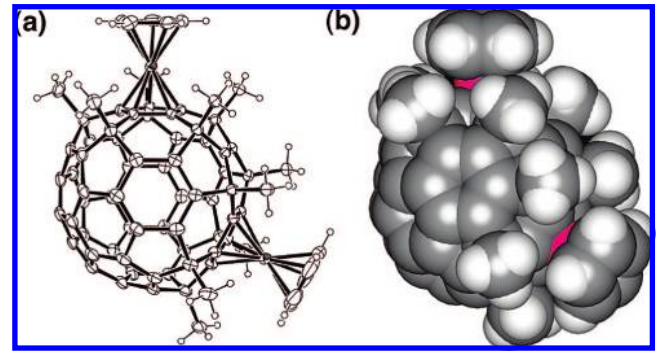

Figure 2. X-ray crystal structure of C_{2v}-$Fe_2(C_{60}Me_{10})Cp_2$. $CHCl_3$ molecules found in a unit cell are omitted for clarity. (a) ORTEP drawing. (b) CPK drawing.

C_{2v} compound is 8.42 Å, which is shorter than that of the D_{5d} compound (9.91 Å). This difference is believed to affect the photophysical properties.

The first insight into fullerene/ferrocene interactions came from quantum chemical calculations at the DFT computational level, which were carried out for the model compounds single-decker buckyferrocene $Fe(C_{60}H_5)Cp$, the highly symmetric D_{5d} and lower symmetric C_{2v} double-decker buckyferrocenes, $Fe_2(C_{60}H_{10})Cp_2$, and their reference compounds. Molecular properties in the ground state — orbital schemes and orbital energies — were evaluated *in vacuo*.

Common to all fullerene/ferrocene donor−acceptor conjugates is a significant d−π conjugation, that is, a 3d orbital (i.e., iron) and σ-/π-orbital (i.e., carbon skeleton of the fullerene) hybridization. Implicit is a weak but noticeable homoconjugation. Closer inspection of the frontier orbitals reveals that the presence of either one or two ferrocene moieties imposes a significant electronic perturbation on the fullerene orbitals. Figure 3 illustrates the HOMO to HOMO-5 and LUMO orbital pictures of the three different buckyferrocenes. Important is that the LUMO in all three of the electron donor−acceptor conjugates is localized on the fullerene core — with a clear separation from the ferrocene fragments — involving the fullerene π-orbital system only. Generally speaking, this confirms that the electron-accepting features of the fullerene are retained despite the degree of functionalization. In the single-decker and highly symmetric D_{5d} double-decker buckyferrocenes, the LUMO is located on the equatorial sites of the fullerene, whereas in the lower symmetric C_{2v} double-decker buckyferrocene, it is localized on the bottom side of the fullerene. This coincides with the LUMO of the references (Figure S1, Supporting Information).

In general, orbital overlaps in the ground-state configuration of all isomers lead to an appreciable redistribution of charge density, namely, charge shift from the electron donor (i.e., ferrocene) to the electron acceptor (i.e., fullerene). The HOMO representations show a fully extended π-conjugation system of the fullerene in all three electron donor−acceptor conjugates, involving increasing contributions from iron 3d atomic orbitals. Interestingly, the C_{2v} isomer is a fully extended 3d−π system, whereas the single-decker compound and D_{5d} isomer reveal only small contributions from the iron orbitals. Taking the lower-lying HOMO orbitals into consideration, remarkable rearrangements of the electron density in comparison to the reference structures are evidenced. Thereby, a charge shift from the fullerene π-electron system to the ferrocene moieties occurs, resulting in a spatial separation of the orbitals between the donor and acceptor. Careful analysis of the orbital energies and their

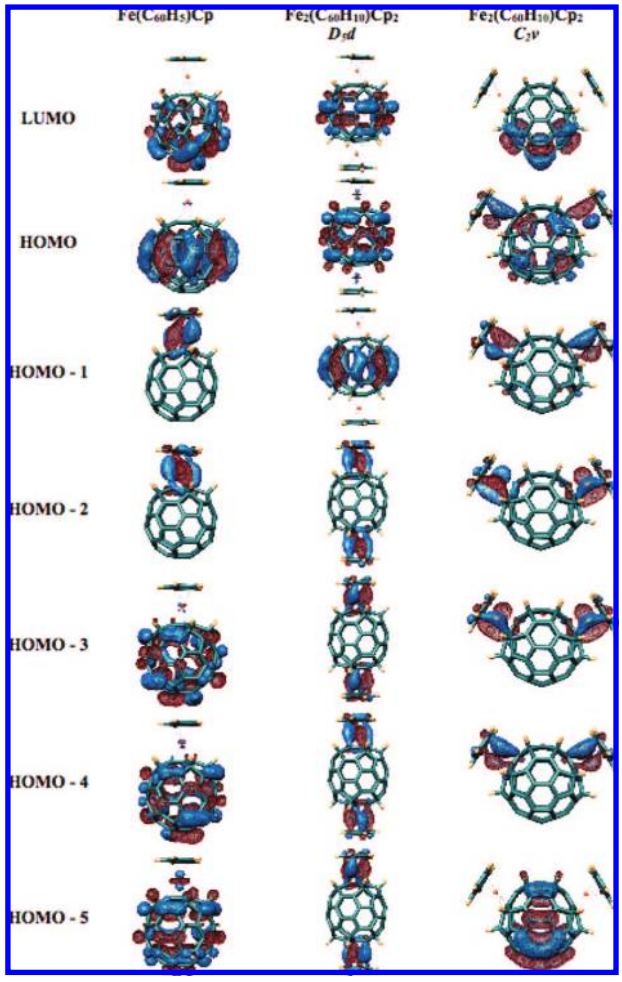

Figure 3. Molecular orbital representations of the single-decker buckyferrocene, $Fe(C_{60}H_5)Cp$, and the highly symmetric D_{5d}- and lower symmetric C_{2v}-$Fe_2(C_{60}H_{10})Cp_2$, obtained by DFT calculations (B3PW91/6-31G*+LANL2DZ). The HOMOs are mainly localized on the ferrocene and separated from the fullerene orbitals, giving rise to measurable charge-transfer properties.

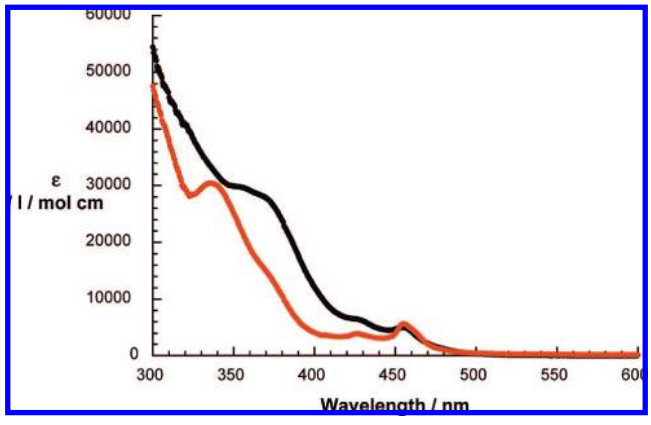

Figure 4. Absorption spectra of double-decker reference systems D_{5d}-$C_{60}Ar_{10}H_2$ (red) and C_{2v}-$C_{60}Ar_{10}H_2$ (black) in toluene.

symmetries further corroborates the donor−acceptor character of these molecules.[11] Thus, photoexcitation of the fullerene facilitates electron transfer from the ferrocene unit to the C_{60}. Similar considerations hold for the D_{5d} and C_{2v} isomers. The D_{5d} buckyferrocene contains two pairs of degenerate HOMO orbitals, namely, HOMO-2/HOMO-3 and HOMO-4/HOMO-5,

Table 1. Orbital Energies (in eV) *in Vacuo* for Single-Decker and Double-Decker Buckyferrocenes, Based on DFT Calculations

	$Fe(C_{60}H_5)Cp$		D_{5d} $Fe_2(C_{60}H_{10})Cp_2$		C_{2v} $Fe_2(C_{60}H_{10})Cp_2$	
	B3PW91/6-31G*+LANL2DZ	B3PW91/6-311+G**+LANL2DZ	B3PW91/6-31G*+LANL2DZ	B3PW91/6-311+G**+LANL2DZ	B3PW91/6-31G*+LANL2DZ	B3PW91/6-311+G**+LANL2DZ
LUMO	−3.18	−3.12	−2.12	−2.08	−2.36	−2.34
HOMO	−6.25	−6.05	−5.65	−5.48	−5.97	−5.83
HOMO-1	−6.26	−6.05	−5.71	−5.54	−6.00	−5.85
HOMO-2	−6.26	−6.05	−5.94	−5.77	−6.01	−5.85
HOMO-3	−6.41	−6.22	−5.95	−5.77	−6.02	−5.86
HOMO-4	−6.41	−6.22	−5.96	−5.79	−6.03	−5.87
HOMO-5	−6.87	−6.70	−5.96	−5.79	−6.18	−6.05

which are entirely separated from the fullerene framework. In the C_{2v} isomers, the degenerate pairs are HOMO-1/HOMO-2 and HOMO-3/HOMO-4. The spatial separation of the ferrocene orbitals from the fullerene core guarantees in all isomers effective charge-transfer properties and affirms the donor character of the ferrocene. Additionally, the significant overlap between the iron atomic orbitals and the carbon framework in the HOMOs of all three systems is ascribed to the presence of endohedral homoconjugation due to weak iron−iron interactions, as found in electrochemistry measurements. This homoconjugation is primarily supported by in-phase interactions between the ferrocene 3d orbitals and the fullerene π-system and provides means for efficient charge transfer from donor to acceptor. In general, we should distinguish between two different processes that evolve from photoexcitation. First, direct excitation into the ferrocene triggers electron-transfer reactions involving the lower-lying occupied orbitals. Second, upon excitation of the fullerene moiety, a locally excited state of C_{60} is generated, from which an electron transfer — involving the well-isolated ferrocene-centered HOMO orbitals and the LUMO (Figure 3) — will evolve. According to the common but oversimplified one-electron concept, transitions across the HOMO−LUMO energy gap would represent a charge-transfer excitation with the following energies (i.e., B3PW91/6-311+G**+LANL2DZ *in vacuo*): 2.92 eV for $Fe(C_{60}H_5)Cp$, 3.39 eV for D_{5d}-$Fe_2(C_{60}H_{10})Cp_2$, and 3.49 eV for C_{2v}-$Fe_2(C_{60}H_{10})Cp_2$. Considering the calculated orbital energies (Table 1), we infer strong electronic couplings between the donor and acceptor fragments. Intimate contacts between the electron acceptor and electron donor are mainly responsible for this trend. Hereby, the LUMO energy of the C_{2v} isomer (−2.34 eV) is slightly lower than that of the corresponding D_{5d} isomer (−2.08 eV), which is in good agreement with the cyclic voltammetry experiments. Additional proof for the electronic coupling came from absorption spectra (*vide supra*), which are not a linear superimposition of the individual reference component spectra. In conclusion, intimate donor−acceptor contacts, as well as the significant shift of charge density from acceptor to donor together with the notable orbital interactions between the ferrocene 3d orbitals and the fullerene π-system, have been confirmed. This is expected to impact the excited-state and the charge-transfer-state characteristics.

To verify that the electron donor−acceptor interactions also prevail in the solution, we turned to electrochemical experiments that were performed in benzonitrile. In general, two oxidative

(11) As evidenced from Figure 3, the HOMO-1 and HOMO-2 orbitals of the mono-adduct are fully localized on the ferrocene residue, reflecting the electron-donating properties of the ferrocene. Furthermore, these two orbitals are symmetric, with degenerate energies that match the HOMO energy.

processes were observed that correspond to the one-electron oxidations of each ferrocene moiety. Although the first oxidation potentials were nearly isomer independent (D_{5d}-$Fe_2(C_{60}Me_{10})Cp_2$, 0.063 V vs Fc/Fc^+; C_{2v}-$Fe_2(C_{60}Me_{10})Cp_2$, 0.048 V vs Fc/Fc^+), the second oxidation potentials reflect the coupling between the two ferrocenes (D_{5d}-$Fe_2(C_{60}Me_{10})Cp_2$, 0.173 V vs Fc/Fc^+; C_{2v}-$Fe_2(C_{60}Me_{10})Cp_2$, 0.183 V vs Fc/Fc^+). The reduction, on the other hand, is shifted to −2.295 V for D_{5d}-$Fe_2(C_{60}Me_{10})Cp_2$ and −2.138 V for C_{2v}-$Fe_2(C_{60}Me_{10})Cp_2$. Relative to the corresponding references, these involve shifts of nearly 0.3 V. Notably, the electrochemistry corroborates the electron-accepting and -donating features of the fullerene and the ferrocene, respectively, despite some anodic shifts. By adding the first oxidation potential and the first reduction potential, the energy of the radical ion pair state is estimated to be about 2.36 eV for D_{5d}-$Fe_2(C_{60}Me_{10})Cp_2$ and 2.21 eV for C_{2v}-$Fe_2(C_{60}Me_{10})Cp_2$ in benzonitrile when neglecting Coulomb interactions; considering Coulomb interactions, we estimate values of 2.24 and 2.09 eV, respectively.

In view of the DFT calculations, we employed a variety of photophysical techniques to quantify the donor−acceptor interactions and probe their outcome. First, the absorption spectra shall be discussed. The spectra show the typical absorption features of fullerenes: strong absorptions in the UV (i.e., maximum at 340 nm and shoulder at 370 nm) and weaker absorptions in the visible (i.e., maxima at 430 and 460 nm) ranges (Figure 4). Spectroscopically relevant is the 0−*0 transition around 460 nm.[12]

A close inspection of the double-decker buckyferrocenes reveals that their absorption spectra fail to be a linear superimposition of the individual component spectra. In particular, additional features are discernible in the range above 460 nm (i.e., 550 nm for D_{5d}-$Fe_2(C_{60}Me_{10})Cp_2$ and 516 nm for C_{2v}-$Fe_2(C_{60}Me_{10})Cp_2$), where neither the fullerenes nor the ferrocenes absorb at all. In line with previous studies we evoke the charge-transfer features (see Figure 5).[8] Importantly, the energies of the charge transfer bands follow the trend seen in the electrochemically derived charge-separated state energies (*vide infra*). Such charge transfer features are primarily a consequence of the strong electronic coupling (V) between the fullerenes and ferrocenes, which determined by[13]

$$V = \frac{2.06 \times 10^{-2} \sqrt{\varepsilon_{max} \nu_{max} \Delta\nu_{1/2}}}{R_{cc}} \quad (1)$$

are 205 and 290 cm^{-1} for the D_{5d}- and C_{2v}-$Fe_2(C_{60}Me_{10})Cp_2$, respectively. For the double-decker buckyferrocenes in toluene, the parameters are as follow: $\epsilon_{max}(D_{5d}) = 72\ M^{-1}\ cm^{-1}$, $\epsilon_{max}(C_{2v}) = 155\ M^{-1}\ cm^{-1}$, $\nu_{max}(D_{5d}) = 18\,182\ cm^{-1}$, $\nu_{max}(C_{2v}) = 19\,380\ cm^{-1}$, $\Delta\nu_{1/2}(D_{5d}) = 1695\ cm^{-1}$, and $\Delta\nu_{1/2}(C_{2v}) = 1620\ cm^{-1}$. According to the results of the geometry optimizations, center-to-center distances (R_{cc}) of 4.96 and 4.94 Å were determined for D_{5d}- and C_{2v}-$Fe_2(C_{60}Me_{10})Cp_2$, respectively.

In summary, assays regarding the ground-state features, including DFT calculations, electrochemistry, and absorption

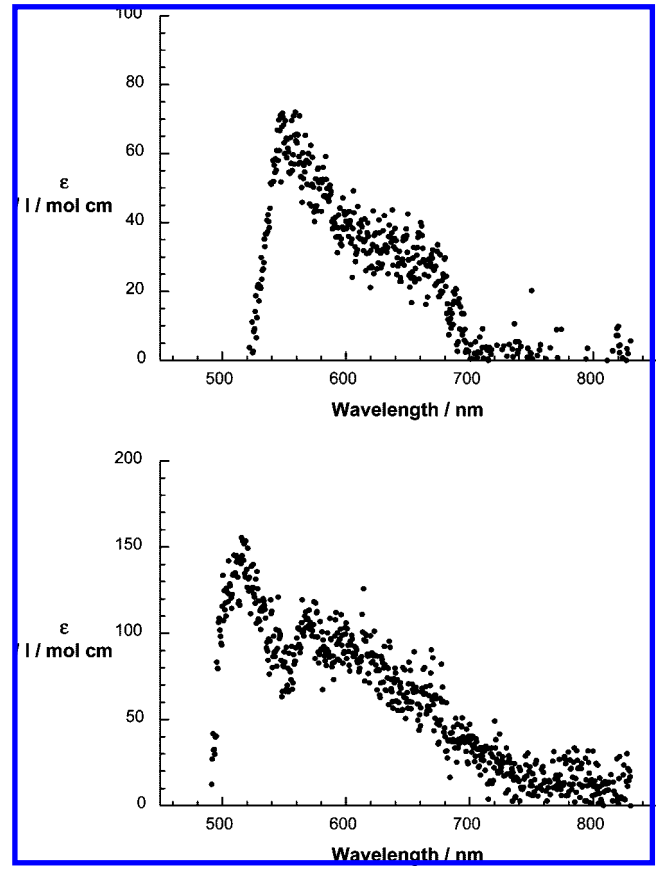

Figure 5. (Top) Charge-transfer band of D_{5d}-$Fe_2(C_{60}Me_{10})Cp_2$ in toluene. (Bottom) Charge-transfer band of C_{2v}-$Fe_2(C_{60}Me_{10})Cp_2$ in toluene. Please note that, in the range above 490 nm, a negative absorption results.

spectroscopy, suggest notable electronic perturbations in the double-decker buckyferrocenes D_{5d}- and C_{2v}-$Fe_2(C_{60}Me_{10})Cp_2$. Implicit is a partial redistribution of charge density from the electron-donating ferrocenes to the electron-accepting fullerene. Of particular interest is also the 700−800 nm range in the charge-transfer absorption of C_{2v}-$Fe_2(C_{60}Me_{10})Cp_2$, which bears close resemblance to an intervalence charge-transfer transition (i.e., ferrocene−ferrocenium interactions) seen in multimetal complexes.[14] In fact, this experimental observation is in line with the molecular orbital calculations, which reveal, in the C_{2v} isomer, the presence of a fully extended 3d−π system exists. Note the lack of this in D_{5d}-$Fe_2(C_{60}Me_{10})Cp_2$, pointing to weak ferrocene−ferrocene coupling across the fullerene moiety.

Next, we employed fluorescence spectroscopic tools — steady-state and time-resolved fluorescence — to probe excited-state deactivation. Both fullerenes that lack electron-donating ferrocenes, that is, D_{5d}- and C_{2v}-$C_{60}Ar_{10}H_2$, emerged hereby as important reference systems. The steady-state fluorescence spectra of the double-decker reference systems, relative to the single-decker reference systems (i.e., $C_{60}R_5H$; R = Me or Ph),[8] show a number of significant differences (Figure 6 and Table 2). First, much higher fluorescence quantum yields (2.1×10^{-1} versus 2.2×10^{-3}) are detected. Second, blue-shifted fluorescence maxima (i.e., 568 and 467 nm for D_{5d}- and C_{2v}-$C_{60}Ar_{10}H_2$, respectively, versus 615 nm) are gathered for the double-decker reference systems. Third, different symmetries (i.e., D_{5d} versus C_{2v}) go along with different fluorescence quantum yields (i.e.,

(12) (a) Matsuo, Y.; Tahara, K.; Morita, K.; Matsuo, K.; Nakamura, E. *Angew. Chem., Int. Ed.* **2007**, *46*, 2844. (b) Sawamura, M.; Kuninobu, Y.; Toganoh, M.; Matsuo, Y.; Yamanaka, M.; Nakamura, E. *J. Am. Chem. Soc.* **2002**, *124*, 9354. (c) Sawamura, M.; Toganoh, M.; Kuninobu, K.; Kato, S.; Nakamura, E. *Chem. Lett.* **2000**, 270. (d) Matsuo, Y.; Muramatsu, A.; Tahara, K.; Koide, M.; Nakamura, E. *Org. Synth.* **2006**, *83*, 80.

(13) Armaroli, N.; Marconi, G.; Echegoyen, L.; Bourgeois, J.-P.; Diederich, F. *Chem. Eur. J.* **2000**, *6*, 1629.

(14) See, for example: D'Alessandro, D. M.; Keene, F. R. *Chem. Soc. Rev.* **2006**, *35*, 424.

Table 2. Photophysical Properties of Single-[8] and Double-Decker Buckyferrocenes

		single-decker buckyferrocene[8]				double-decker buckyferrocene			
						D_{5d}		C_{2v}	
	solvent	$C_{60}Me_5H$	$Fe(C_{60}Me_5)Cp$	$C_{60}Ph_5H$	$Fe(C_{60}Ph_5)Cp$	$C_{60}Ar_{10}H_2$	$Fe_2(C_{60}Me_{10})Cp_2$	$C_{60}Ar_{10}H_2$	$Fe_2(C_{60}Me_{10})Cp_2$
fluorescence quantum yield (Φ)	toluene	2.2×10^{-3}	2.4×10^{-5}	1.5×10^{-3}	3.3×10^{-5}	2.1×10^{-1}	7.2×10^{-5}	6.1×10^{-2}	2.2×10^{-4}
	THF	2.2×10^{-3}	1.6×10^{-5}	1.4×10^{-3}	2.6×10^{-5}	1.5×10^{-1}	7.7×10^{-5}	4.7×10^{-2}	2.1×10^{-4}
fluorescence lifetime (τ)	toluene	710 ps		650 ps		95 ns		1.2 ns	
	THF	690 ps		585 ps		83 ns		1.0 ns	
singlet (τ)	toluene	705 ps	0.8 ps	615 ps	0.9 ps	~90 ns	0.77 ps	1.2 ns	0.74 ps
	THF	650 ps	0.7 ps	550 ps	0.7 ps	~90 ns	0.72 ps	1.0 ns	0.57 ps
radical ion pair (τ)	toluene		35 ps		39 ps		18.9 ps		17.0 ps
	THF		28 ps		27 ps		11.8 ps		14.7 ps
	bzcn				21 ps		8.6 ps		11.6 ps

2.1×10^{-1} versus 6.1×10^{-2}). From the average difference between the long-wavelength absorption (i.e., 464 nm) and the short-wavelength fluorescence (i.e., 568 and 467 nm for D_{5d}- and C_{2v}-$C_{60}Ar_{10}H_2$, respectively), we derive singlet excited-state energies of 2.4 eV for D_{5d}-$C_{60}Ar_{10}H_2$ and 2.7 eV for C_{2v}-$C_{60}Ar_{10}H_2$.

When comparing the fluorescence of the double-decker buckyferrocenes with that of the reference systems (Figure 6), a significant quenching of the fullerene-centered fluorescence is observed around 568 and 467 nm for the D_{5d}- and C_{2v}-$Fe_2(C_{60}Me_{10})Cp_2$, respectively. On the basis of such a quenching, we might expect rapid singlet excited-state deactivations, which is in line with the spatially close donor−acceptor separations and the strong electronic couplings (*vide supra*). In parallel with the 467 nm fluorescence quenching of the fullerene, we noticed new fluorescence features in the red region. More precisely, 650 and 560 nm peaks evolve for D_{5d}- and C_{2v}-$Fe_2(C_{60}Me_{10})Cp_2$, respectively. A likely rationale implies rather strong charge-transfer emission with quantum yields of around 10^{-3} that mirror image the charge-transfer absorptions at 550 and 516 nm.

Insight into the fluorescence dynamics came from time-resolved fluorescence decay spectroscopy, where lifetimes of 95 (D_{5d}-$C_{60}Ar_{10}H_2$) and 1.18 ns (C_{2v}-$C_{60}Ar_{10}H_2$) were determined for the two reference systems (Table 2). In other words, excited-state deactivations in the double-decker reference systems (40 π-electrons) proceed apparently slower than what has been typically seen in the corresponding single-decker reference systems (50 π-electrons) (Table 2), an observation that is in line with the stronger fluorescence features.[8] Notable is the difference between D_{5d}- and C_{2v}-$C_{60}Ar_{10}H_2$. The ferrocene conjugates, on the other hand, fail to generate any detectable fluorescence within the experimental time resolution of our instrument. Consequently, we must assume that the deactivation is significantly faster than 100 ps.

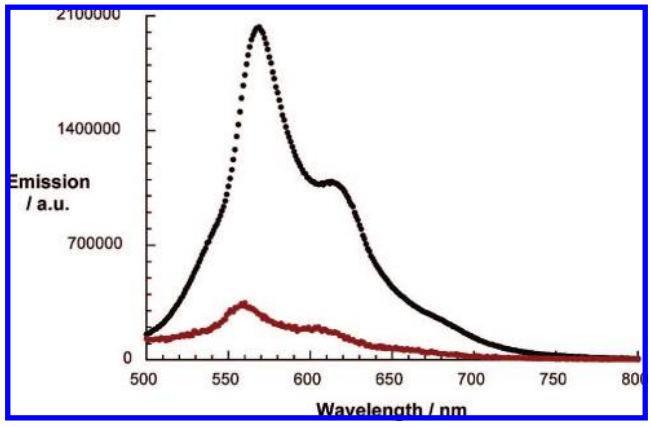

Figure 6. Room-temperature fluorescence spectra of D_{5d}-$Fe_2(C_{60}Me_{10})Cp_2$ (red) and D_{5d}-$C_{60}Ar_{10}H_2$ (black) in toluene, recorded with solutions that exhibit optical absorption of 0.14 at the 400 nm excitation wavelength. Note that the fluorescence spectrum of D_{5d}-$Fe_2(C_{60}Me_{10})Cp_2$ is amplified by a factor of 336.

To shed light on the nature of the product evolving from this intramolecular deactivation, complementary transient absorption measurements were necessary (i.e., with femtosecond through millisecond time resolution). Following the time evolution of the characteristic singlet excited-state features of C_{60}, for instance, is a convenient mode to identify spectral features of the resulting photoproducts and to determine absolute rate constants for the intramolecular decay. This also complements the photophysical analysis of the single-decker buckyferrocenes and the corresponding references systems by expanding the wavelength range to the relevant near-infrared region.[8]

Up front, the excited-state properties of the reference systems, that is, $C_{60}Me_5H$ and $C_{60}Ph_5H$ as well as D_{5d}- and C_{2v}-$C_{60}Ar_{10}H_2$/$C_{60}Ar_{10}H_2$, shall be discussed, since they emerge as important reference points for the interpretation of the features expected in the single-decker and double-decker buckyferrocenes.

Figure 7 illustrates, for example, the differential absorption changes that were recorded in the visible and the near-infrared region spectra upon 387 nm photoexcitation of the single-decker reference $C_{60}Ph_5H$. Commencing with the conclusion of the photoexcitation, excited-state features are seen, especially in the near-infrared region, where distinct maxima evolve at 915 nm. The visible regions, on the other hand, are dominated by maxima at 585 nm. These spectral attributes are indicative of the $C_{60}Me_5H$ and $C_{60}Ph_5H$ singlet excited states. Their decay follows clean first-order kinetics and results in the formation of a sharp absorption around 660 nm, as shown in Figure 7. Multiwavelength analyses of the singlet decays reveal lifetimes of 705 ps for $C_{60}Me_5H$ and 615 ps for $C_{60}Ph_5H$. Importantly, these decay kinetics parallel exactly the growth kinetics at 660 nm. Consequently, we hypothesize the occurrence of intersystem crossing processes to afford the energetically lower-lying triplet excited states. The differential absorption changes, recorded immediately after an 8 ns pulse, showed the same spectral

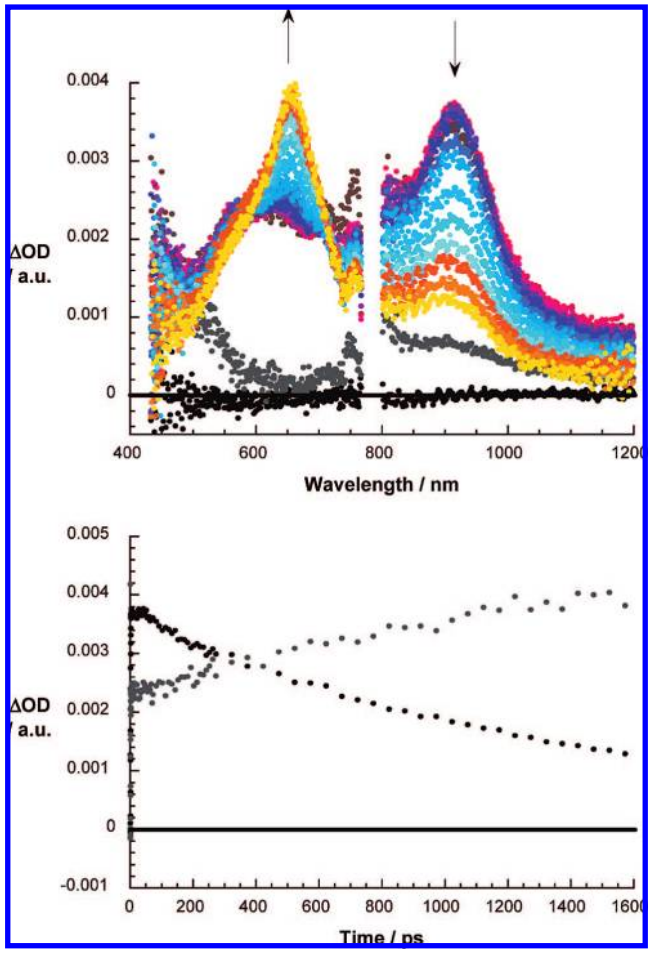

Figure 7. (Top) Differential absorption spectra (visible and near-infrared) obtained upon femtosecond flash photolysis (387 nm) of $C_{60}Ph_5H$ in argon-saturated toluene with several time delays between 0 and 1600 ps at room temperature. Arrows indicate the temporal evolution. (Bottom) Time−absorption profiles of the spectra shown above at 660 and 915 nm, monitoring the singlet-to-triplet intersystem crossing.

features of the $C_{60}Me_5H$ and $C_{60}Ph_5H$ triplet excited states as observed at the end of the femtosecond experiments. To be precise, maxima located at 660 nm were observed. In the absence of molecular oxygen, the triplet lifetime of both single-decker references is about 14 μs.[8] In the presence of molecular oxygen, however, an efficient energy transfer takes place that leads to the quantitative generation of cytotoxic singlet oxygen.[15]

Turning to the double-decker reference systems (i.e., D_{5d}- and C_{2v}-$C_{60}Ar_{10}H_2$), the differential absorption changes recorded immediately after the 387 nm photoexcitation are, in analogy with $C_{60}Me_5H$ and $C_{60}Ph_5H$, ascribed to the formation of the excited singlet states of the two different reference systems. The singlet excited state, displaying distinctive singlet−singlet transitions around 485, 570, and 870 nm for D_{5d}-$C_{60}Ar_{10}H_2$ and 580 and 900 nm for C_{2v}-$C_{60}Ar_{10}H_2$, undergoes quantitative intersystem crossing, for which lifetimes of >3200 and 1232 ps were determined for D_{5d}- and C_{2v}-$C_{60}Ar_{10}H_2$, respectively, to transform the singlet excited state into the energetically lower-lying triplet excited state (Figures 8 and S2, Supporting Information). Again, these lifetimes are in agreement with the fluorescence lifetimes (see Table 2). In the complementary recorded nanosecond spectra (see Figure 9), we see only the

(15) Guldi, D. M.; Prato, M. *Acc. Chem. Res.* **2000**, *33*, 695.

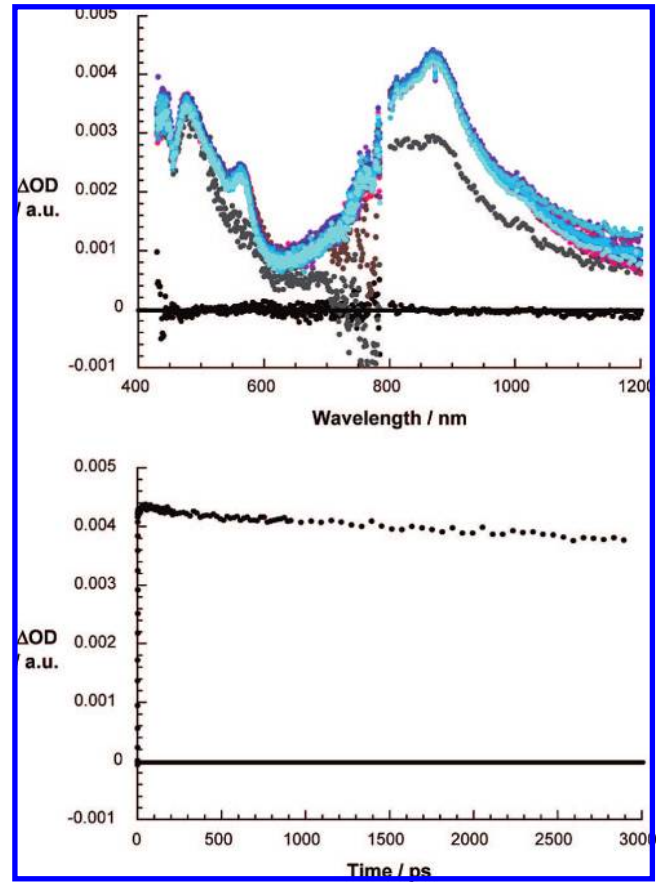

Figure 8. (Top) Differential absorption spectra (visible and near-infrared) obtained upon femtosecond flash photolysis (387 nm) of D_{5d}-$C_{60}Ar_{10}H_2$ in argon-saturated toluene with several time delays between 0 and 3000 ps at room temperature. (Bottom) Time−absorption profile of the spectra shown above at 900 nm, monitoring the singlet-to-triplet intersystem crossing.

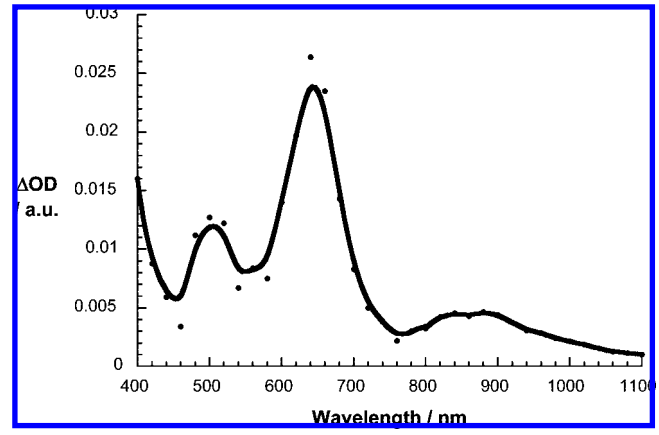

Figure 9. Differential absorption spectrum (visible range) obtained upon nanosecond flash photolysis (337 nm) of D_{5d}-$C_{60}Ar_{10}H_2$ in nitrogen-saturated toluene with a 200 ns time delay at room temperature.

long-lived triplet−triplet transitions for D_{5d}- and C_{2v}-$C_{60}Ar_{10}H_2$. Under anaerobic conditions, the triplet lifetimes are ca. 20 μs. Both triplet excited states turned out to be quite sensitive to oxygen and are quenched with nearly diffusion-controlled kinetics to afford the formation of singlet oxygen.

The instantaneous growth of the 915 nm absorption affirms the successful fullerene excitation in the single-decker buckyferrocenes (i.e., $Fe(C_{60}Me_5)Cp$ and $Fe(C_{60}Ph_5)Cp$) (compare Figures 7 and 10). However, instead of exhibiting slow

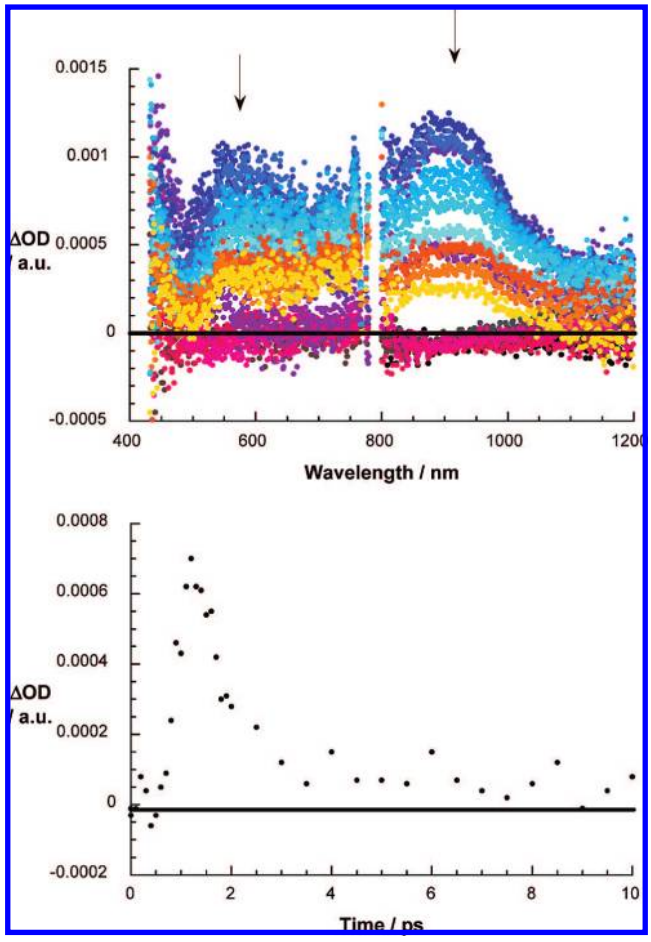

Figure 10. (Top) Differential absorption spectra (visible and near-infrared) obtained upon femtosecond flash photolysis (387 nm) of $Fe(C_{60}Ph_5)Cp$ in argon-saturated toluene with several time delays between 0 and 20 ps at room temperature. Arrows indicate the temporal evolution. (Bottom) Time−absorption profiles of the spectra shown above at 620 nm, monitoring the formation and decay of the radical ion-pair state.

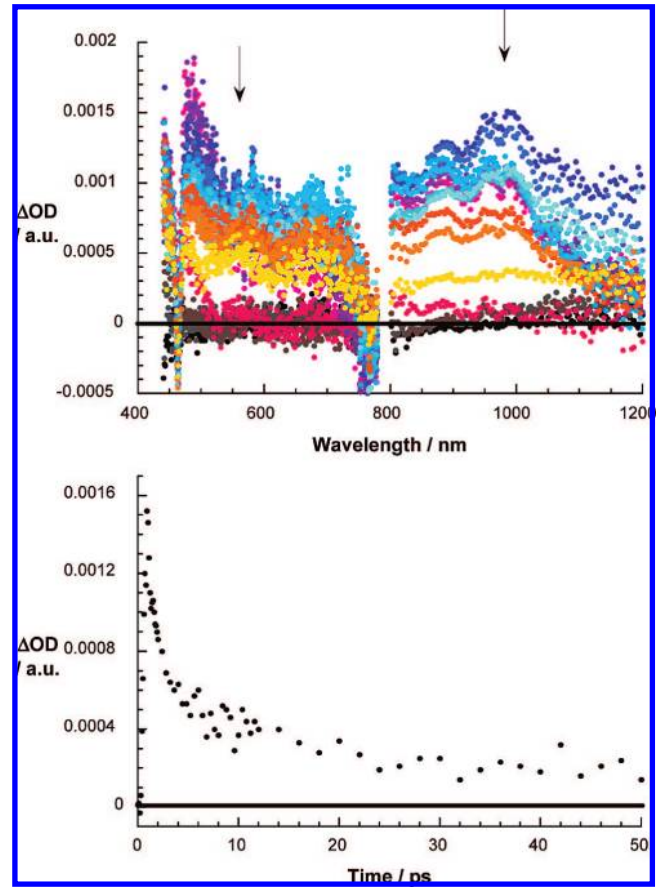

Figure 11. (Top) Differential absorption spectra (visible and near-infrared) obtained upon femtosecond flash photolysis (387 nm) of D_{5d}-$Fe_2(C_{60}Me_{10})Cp_2$ in argon-saturated toluene with several time delays between 0 and 20 ps at room temperature. Arrows indicate the temporal evolution. (Bottom) Time−absorption profiles of the spectra shown above at 600 nm, monitoring the formation and decay of the radical ion pair state.

intersystem crossing dynamics, the singlet−singlet absorption decays in the presence of the ferrocene donors with accelerated dynamics. The singlet excited-state lifetimes, determined from the average of first-order fits of the time−absorption profiles at various wavelengths, are listed in Table 2. Singlet lifetimes of 0.9 ± 0.1 and 0.7 ± 0.1 ps were determined in toluene and THF, respectively. Spectroscopically, the transient absorption changes, taken after the completion of the decay, bear no resemblance to the fullerene triplet excited state. In particular, the new transients reveal maxima at 550 nm/900 and 680 nm, which are ascribed to the one-electron-reduced fullerene and the one-electron-oxidized ferrocene.

Important in this context is that complementary pulse radiolysis reduction experiments with the single-decker reference systems (i.e., $C_{60}Me_5H$ and $C_{60}Ph_5H$) reveal a 545 nm maximum in the visible range. In accordance with these results, we propose that charge separation from the fullerene singlet excited state creates the $Fe^{\bullet+}(C_{60}{}^{\bullet-}R_5)Cp$ state, which is responsible for the fast deactivation of the photoexcited chromophore. All radical ion-pair lifetimes, which are in the order of 30 ± 5 ps, reveal stabilization in the nonpolar environments (i.e., toluene versus THF). Slightly shorter lived is the radical ion-pair state in benzonitrile (i.e., 21 ± 5 ps).

Both double-decker buckyferrocenes (i.e., D_{5d}- and C_{2v}-$Fe_2(C_{60}Me_{10})Cp_2$) show — initially after laser excitation — differential absorption characteristics that resemble those seen in the reference systems, that is, the fullerene singlet−singlet attributes (see Figure 11). In particular, the following maxima evolve: for D_{5d}-$Fe_2(C_{60}Me_{10})Cp_2$, 485, 570, and 885 nm; for C_{2v}-$Fe_2(C_{60}Me_{10})Cp_2$, 600 and 890 nm. In contrast to the double-decker reference systems, we noted, however, a rapid deactivation of the fullerene singlet excited state in $Fe(C_{60}Me_5)Cp$ and $Fe(C_{60}Ph_5)Cp$. More precisely, singlet lifetimes of 0.7 ± 0.05 and 0.6 ± 0.1 ps were determined in toluene and THF, respectively. Features of the new products, as shown in Figures 11 and S3 (Supporting Information), involve transient maxima at 440 and 600 nm (C_{2v}-$Fe_2(C_{60}Me_{10})Cp_2$), as well as transient maxima at 480 and 700 nm plus a broad absorption that ranges from 1000 to 1200 nm (D_{5d}-$Fe_2(C_{60}Me_{10})Cp_2$). The fast deactivations seen for the single-decker and double-decker buckyferrocenes are a consequence of strong electronic coupling between electron donor (i.e., ferrocene) and photoexcited electron acceptor (i.e., fullerene).

A decisive interpretation of the spectral changes that are seen at the conclusion of the rapid singlet decay (Figures 11 and S3) requires, however, a comparison with spectroelectrochemical and pulse radiolytic investigations. Both techniques were meant to shed light on absorption features of the one-electron-reduced fullerenes. Reduction of D_{5d}-$Fe_2(C_{60}Me_{10})Cp_2$ was accomplished with a slight excess of potassium in THF under anaerobic conditions.[9] The course of the reaction is accompanied by a color change from yellow to light green. In line with previous

work, this one-electron reduction led to marked changes in the UV−vis−NIR spectra: new absorption maxima at 505, 750 and 1190 nm.[16] Pulse radiolytic reduction, on the other hand, was performed to selectively reduce C_{2v}-$Fe_2(C_{60}Me_{10})Cp_2$. A solvent mixture containing toluene, 2-propanol, and acetone was used, where in the absence of molecular oxygen strongly reducing $(CH_3)_2{}^{\bullet}COH$ and $(CH_3)_2{}^{\bullet}CO^-$ radicals were formed that were sufficiently reactive to reduce electron acceptors such as C_{60} and a number of fullerene derivatives. The differential absorption spectrum following the conclusion of the radiolytic reduction of C_{2v}-$Fe_2(C_{60}Me_{10})Cp_2$ is shown in Figure S4 (Supporting Information). Sets of maxima at 430 and 570 nm and a minimum at 460 nm are clearly discernible that are formed under pseudo-first-order conditions.

When considering the features of the radiolytically generated C_{2v}-$Fe_2(C_{60}{}^{\bullet-}Me_{10})Cp_2$ and the chemically generated D_{5d}-$Fe_2(C_{60}{}^{\bullet-}Me_{10})Cp_2$, we note in the 400−1200 nm range of the photoexcited double-decker buckyferrocenes (i.e., D_{5d}- and C_{2v}-$Fe_2(C_{60}Me_{10})Cp_2$), on femto- and picosecond time scales, transitions of the one-electron-reduced radical anion of the fullerene and the one-electron-oxidized radical cation of the ferrocenes. Interestingly, the lifetimes of the charge-separated states are placed in the inverted region of the Marcus parabola with values that are typically longer (i) in less polar toluene than in more polar THF and than in even more polar benzonitrile, as well as (ii) in D_{5d}-$Fe_2(C_{60}Me_{10})Cp_2$ than in C_{2v}-$Fe_2(C_{60}Me_{10})Cp_2$. Implicit is that both trends promote higher energies of the charge-separated states. Nevertheless, all of these values are notably lower than what has been determined for the corresponding single-decker buckyferrocenes.

(16) (a) Guldi, D. M. *J. Phys. Chem. A* **1997**, *101*, 3895. (b) Guldi, D. M.; Hungerbühler, H.; Asmus, K.-D. *J. Phys. Chem. A* **1997**, *101*, 1783.

Conclusions

This work shows that, in both single- (i.e., $Fe(C_{60}R_5)Cp$, R = Me, Ph) and double-decker buckyferrocenes (i.e., D_{5d}- and C_{2v}-$Fe_2(C_{60}Me_{10})Cp_2$), significant electronic perturbations of the fullerene electronic structure by the ferrocene, due to orbital overlaps between the fullerene and the ferrocene, as well as the intimate contact between the donor and the acceptor, lead to ultrafast singlet excited-state deactivation and a measurable but short-lived charge-transfer reaction. The addition of the second ferrocene leads in one particular case, namely that of C_{2v}-$Fe_2(C_{60}Me_{10})Cp_2$, to intervalence charge-transfer interactions and increases the reorganization energy of the corresponding double-decker buckyferrocenes, resulting in shorter radical ion-pair lifetimes in comparison to the single-decker buckyferrocenes.

Acknowledgment. Generous support for this collaborative research from the Alexander von Humboldt Foundation (to E.N. and S.S.G.) is gratefullyly acknowledged. The SFB 583, DFG (GU 517/4-1), FCI, and the Office of Basic Energy Sciences of the U.S. Department of Energy are acknowledged for their financial support. We dedicate this paper to Professor Horst Kisch on the occasion of his retirement.

Supporting Information Available: CIF file for the crystal structure of the C_{2v}-double-decker buckyferrocene; molecular orbital representation of the reference compounds and transient absorption spectra including pulse radiolysis; complete ref 10. This material is available free of charge via the Internet at http://pubs.acs.org.

JA8013902